

CFD ANALYSIS OF THE AERODYNAMIC RESPONSE OF A TWIN-BOX DECK CONSIDERING DIFFERENT GAP WIDTHS

Rubén Sánchez¹, Félix Nieto^{1*} Kenny C.S. Kwok² and Santiago Hernández¹

1: Structural Mechanics Research Group
School of Civil Engineering
University of La Coruña
Campus de Elviña s/n, 15071 La Coruña, Spain.
e-mail: ruben.sanchez.fernandez@gmail.com; {felix.nieto, santiago.hernandez}@udc.es
web: <http://www.gme.udc.es>

2: Institute for Infrastructure Engineering
University of Western Sydney
Penrith (Kingswood) 2751, Australia.
e-mail: k.kwok@uws.edu.au

Keywords: CFD, URANS, Twin-box deck, force coefficients, vortex shedding, aerodynamics

Abstract *Twin-box bridge decks offer a very good aeroelastic response in terms of flutter stability. Because of this, they are being adopted in some of the most challenging long span bridges recently built such as the Stonecutters or the Xihoumen Bridges. On the other hand, this configuration is particularly prone to vortex induced vibration, since vortices shed from the windward box can impinge on the leeward box causing important oscillations when exciting any of the natural frequencies of the structure. The aim of this work is to study the ability of 2D URANS models to correctly reproduce the effect of the gap width in the force coefficients and the vortex shedding of the static twin-box decks. The numerical results are compared with the experimental data obtained by means of wind tunnel tests of a sectional model considering arrangements with different gap-widths. It has been found that the simulations can reproduce with good accuracy the experimental force coefficients for five different gap widths in the range of angles of attack (-10° , $+10^\circ$). In the same manner, the Strouhal number agrees well with the experimental data reported in the literature. Finally, the distributions of the mean pressure coefficients around deck configurations, based on the gap width, are also reported.*

1. INTRODUCTION

Multi-box and, particularly, twin-box decks, have received growing attention in recent years. The need for spanning longer distances has demanded a particularly efficient aeroelastic response from bridge deck designs. Multi-box bridge decks have proved to provide better

aeroelastic responses that their single deck counterparts [1]. On the other hand, multi-box bridge deck arrangements have shown to be prone to vortex-induced vibrations which must be carefully tackled [2, 3, 4]. Remarkable examples of twin-box bridges recently built are the Xihoumen Bridge, which is a suspension bridge with a main span of 1650 m and the Stonecutters Bridge, a cable-stayed bridge with an impressive 1018 m main span length.

One of the most important parameters influencing the aerodynamic and aeroelastic response of twin-box decks is the gap distance between boxes. With the aim of studying the effect of the gap width, several experimental works, such as [5, 6, 7 and 8] have been published. In the aforementioned references it is noted the complexity of the flow around the twin-box girder and the dramatic effect of the gap width in the aerodynamic response. It is clear that wind tunnel campaigns studying the gap width effect are technically complex and require substantial resources in terms of funding, time, facilities and skilled staff. Moreover, only a limited number of gap widths can be tested.

CFD based simulations have shown their potential in wind engineering based design of bridge decks [9, 10]. The goal of this work is to explore the capability of relatively inexpensive 2D URANS simulations to identify the changes in the aerodynamic response of twin-box decks as a function of the gap width. Instead of aiming at perfectly matching wind tunnel results, for which cumbersome 3D simulations using DES or LES turbulence models would be required, the focus has been put on the changes in the overall aerodynamic response for different gap widths. From a practical point of view, these simulations should pertain to the initial design stage, at which a certain gap distance should be fixed in order to advance along the design process, reserving wind tunnel test campaigns for the final design of the definitive bridge deck arrangement.

In this work the numerical simulations are validated with the experimental data reported in [7]; therefore, the same deck geometry and gap separations between boxes are considered. The reported data are: force coefficients in the range of angles of attack between (-10° and +10°), distribution around the boxes of the mean pressure coefficients and the standard deviation of the pressure coefficients, vortex shedding frequency for the fixed deck. The numerical results agree well with the wind tunnel data confirming the feasibility of the proposed approach.

2. NUMERICAL FORMULATION

The time averaging of the equations for conservation of mass and momentum gives the Reynolds averaged equations of motion in conservation form (Wilcox, 2006).

$$\frac{\partial U_i}{\partial x_i} = 0 \quad (1)$$

$$\rho \frac{\partial U_i}{\partial t} + \rho U_j \frac{\partial U_i}{\partial x_j} = -\frac{\partial P}{\partial x_i} + \frac{\partial}{\partial x_j} (2\mu S_{ij} - \rho \overline{u'_i u'_j}) \quad (2)$$

where U_i is the mean velocity vector, x_i is the position vector, t is the time, ρ is the fluid density, u'_i is the fluctuating velocity and the over-bar represents the time average,

P is the mean pressure, μ is the fluid viscosity and S_{ij} is the mean strain-rate tensor. From the former equation, the specific Reynolds stress tensor is defined as:

$$\tau_{ij} = -\overline{u'_i u'_j} \quad (3)$$

which is an additional unknown to be modelled based on the Boussinesq assumption for one and two equation turbulence models (Wilcox, 2006).

$$\tau_{ij} = 2\nu_T S_{ij} - \frac{2}{3}k\delta_{ij} \quad (4)$$

where ν_T is the kinematic eddy viscosity, S_{ij} is the mean strain-rate tensor and k is the kinetic energy per unit mass of the turbulent fluctuation.

In this work the closure problem is solved applying the two-equation Menter's $k-\omega$ SST model for incompressible flows (Menter and Esch, 2001). The CFD solver of choice has been OpenFOAM.

3. GEOMETRY AND COMPUTER MODELING

3.1. Cross-section geometry

The geometry of the bare cross-section of the considered twin-box deck is depicted in figure 1, which resembles the one of the Stonecutters Bridges. In this work appendages such as barriers, maintenance gantry rails or aerodynamic devices, such as guide vanes, have not been included in the model since the focus has been put on the effect in the aerodynamic response caused by the separation between deck boxes. In a similar manner, since a 2D approach has been chosen for the numerical simulations, no transverse beams connecting the twin boxes have been included.

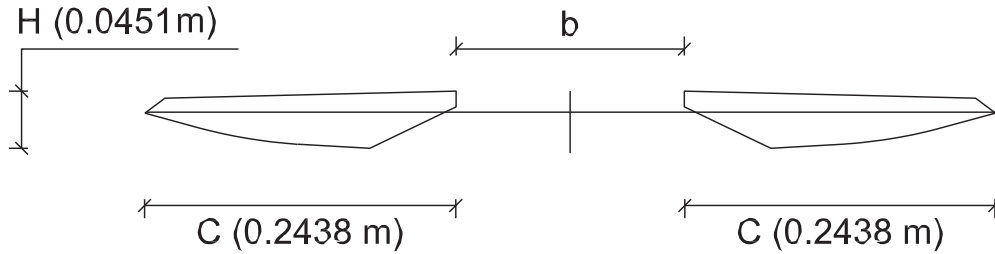


Figure 1. Twin-box deck geometry.

Five different arrangements in terms of gap distance between boxes have been considered, being the ratio of the gap width b to the total deck width B (inside the parenthesis the ratio of the gap width b to the deck depth H is also provided): 0% (0), 2.5% (0.3), 16% (2.1), 27% (4.1) and 35% (6). These five configurations are the same that were studied by means of wind tunnel tests by Kwok and co-workers [7] and in the following they are named as

Gap 1, *Gap 2*,...and *Gap 5*. It must be noted that the actual configuration of the Stonecutters Bridge corresponds to *Gap 4*. The geometric scale considered herein is 1:80, consistent with the experimental tests reported in the aforementioned reference.

3.2. Computational domain and finite volume mesh

A 2D non-structured grid, based on quadrangular elements, has been produced for the 2D URANS simulations which are going to be reported next. The overall shape of the fluid domain is parabolic and an image is provided in figure 2. In the figure, the dimensions of the fluid domain are provided in terms of C which is the single box width. Four different regions have been considered in order to control the cells size and the grid density: Outer region (*OR*), Wake (*W*), Near Wall (*NW*) and Boundary Layer (*BL*).

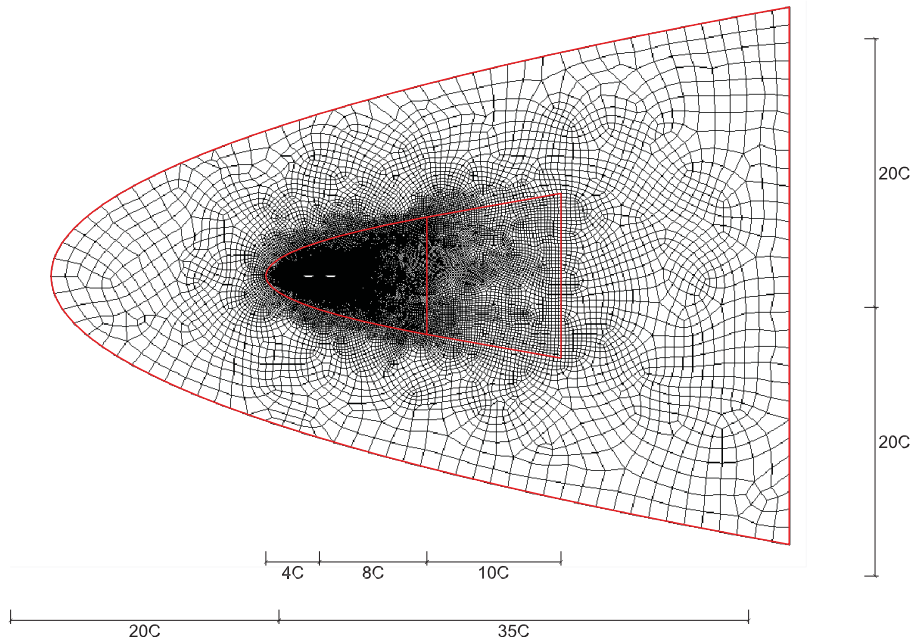


Figure 2. Flow domain general view.

The boundary layer mesh, that is, the structured mesh attached to the body surface is of great importance since it must be capable of accurately simulate the behaviour of the viscous boundary layer, and particularly separation and reattachment phenomena. In this work, instead of wall functions whose use, according to Blazek [11], is questionable for separated flows, a low Reynolds approach has been preferred. For the boundary layer mesh, 21 layers with a growth ratio of 1.12 have been defined. The height of the first layer is about $1 \times 10^{-4} C$. The maximum time-averaged non-dimensional height of the first layer of cells ($y^+ = (U_\tau y_p) / \nu$ where U_τ is the friction velocity, y_p is the first cell height and ν is the kinematic viscosity) is about 6, which is below the usually accepted limit of 8.

Uniform flow velocity of 15 m/s has been imposed at the fluid domain inlet (parabolic external bound in figure 2). In the same manner low turbulence uniform values were set for k and ω at the inlet. A uniform pressure outlet at atmospheric pressure was set at the right bound of the fluid domain. The deck has been modelled as static non-slip walls.

For the same flow domain several meshes with different grid densities have been studied in order to identify the mesh with lower computational demands providing accurate results when compared with the available experimental data of the *Gap 4* case. This is particularly important since the force coefficients reported next are obtained from 55 different unsteady simulations. The overall number of cells for the selected *Gap 4* model grid has been 133107.

4. FORCE COEFFICIENTS

The definition of the force coefficients in this work is the following:

$$C_D = \frac{D}{\frac{1}{2}\rho U^2 B} \quad C_L = \frac{L}{\frac{1}{2}\rho U^2 B} \quad C_M = \frac{M}{\frac{1}{2}\rho U^2 B^2} \quad (5)$$

In the former expressions, D is the drag force per span length, positive windward, L is the lift force per span length, positive upwards, and M is the twist moment per unit of span length, positive in the clock-wise direction. In figure 3 the force coefficients of the five different gap widths considered in this work are provided for the range of angles of attack (-10° , $+10^\circ$). The computer simulations reported herein correspond to angles of attack of -10° , -8° , -6° , -4° , -2° , 0° , 2° , 4° , 6° , 8° and 10° . Positive angles of attack correspond to “nose-up” positions of the deck, facing the incoming flow.

Force coefficients provide an initial assessment of the aerodynamic and aeroelastic performance of the deck. The mean wind load on the deck can be obtained from the force coefficients, and the slopes of the lift and moment coefficient must be positive and have small values, which are indicative of good aeroelastic behaviour.

From figure 3 it can be appreciated the good agreement of the numerical simulations with the experimental wind tunnel tests. Some discrepancies can be identified in the lift and moment coefficients for *Gaps 3,4* and 5. In this respect, it must be borne in mind that the 2D URANS simulations do not include the transversal beams connecting at regular intervals the two boxes of the deck. On the contrary, the sectional model in Kwok et al. [7] does include transversal beams; hence some discrepancies for the bigger gaps must have been expected since the surface of the transverse beams exposed to the flow is bigger.

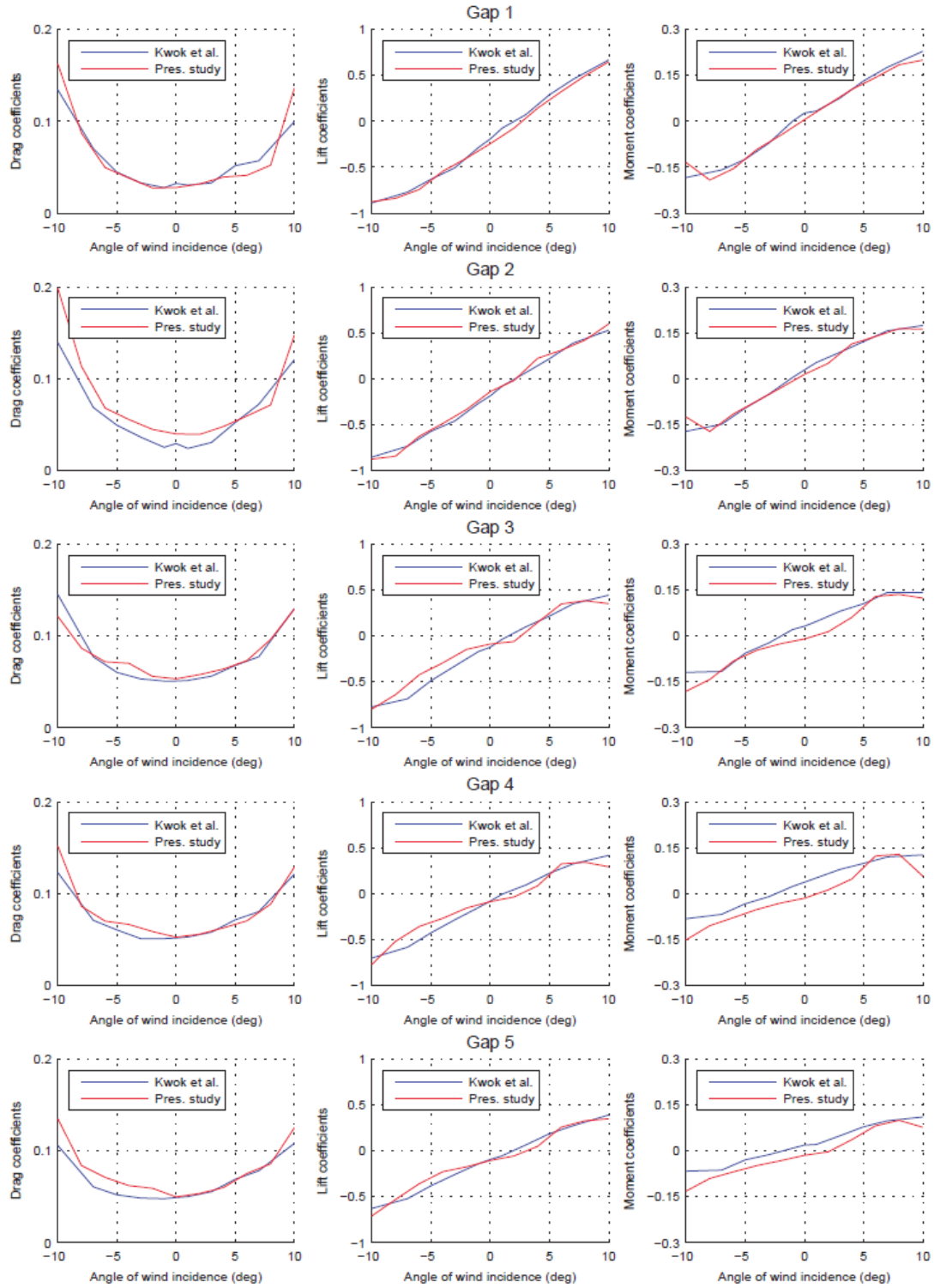


Figure 3. Force Coefficients.

5. VORTEX SHEDDING

In this section the main findings concerning the shedding of vortices from the static deck cross-section are reported. Undesired vortex-induced vibrations of the bridge deck can be caused by the shedding of vortices from the deck boxes. Vortex shedding is usually described from the non-dimensional frequency known as Strouhal number:

$$S_t = \frac{fH}{U} \quad (6)$$

Where f is the vortex shedding frequency, H is the deck depth and U is the undisturbed flow velocity.

In table 1 the Strouhal numbers obtained from the spectra of the lift force time histories of the five considered gap arrangements are reported. The agreement between numerical and experimental data is remarkably good, finding non-negligible differences only for *Gap 2*. For *Gap 1* no vortex shedding has been identified since no peak in the spectrum of the lift coefficient has been identified.

Case	Present study	Experiment [7]
<i>Gap 1</i>	----	----
<i>Gap 2</i>	0.10	0.13
<i>Gap 3</i>	0.24	0.23
<i>Gap 4</i>	0.26	0.27
<i>Gap 5</i>	0.27	0.28

Table 1. Strouhal number: Numerical and experimental data.

In figure 4 the results reported in table 1 are plotted along with the experimental ones published by Laima and Li [8] for a twin-box deck with the geometry of the Xihoumen Bridge. It can be appreciated the consistency among them (the offset in the values is due, mainly, to the difference in the deck depth, H , of the sectional model in [8] compared to the model in [7]). In figure 4, *Region 1* and *Region 2* described in [8] are also identified. In *Region 1*, which is identified in [8] for a gap ratio $b/H \leq 2.138$, the Strouhal number decreases sharply with the gap ratio. On the other hand, in *Region 2*, which corresponds to gap ratios $b/H \geq 2.138$, is characterized by an strong increment in the Strouhal number close to the critical gap ratio and a tendency to reach a constant value for gap ratios higher than 5. Focusing now on the vortex shedding qualitative characteristics, in *Region 1* the shear layers coming from the windward box cross over the gap between boxes and alternate vortex shedding takes part in the wake of the leeward box. On the other hand, in *Region 2*, the shear layers that come from the windward box roll up into the gap and vortices are shed, which impinge on the downstream box (this phenomenon has also been qualitatively described in [12]). In figure 5, instantaneous vorticity fields are provided for *Gap 2* and *Gap 4*, characteristic of *Region 1* and *Region 2* respectively, depicting the aforementioned flow patterns. This fact points towards the general validity of the proposed regions in terms of vortex shedding characteristics, but also shows the ability of relatively inexpensive 2D URANS simulations to identify these.

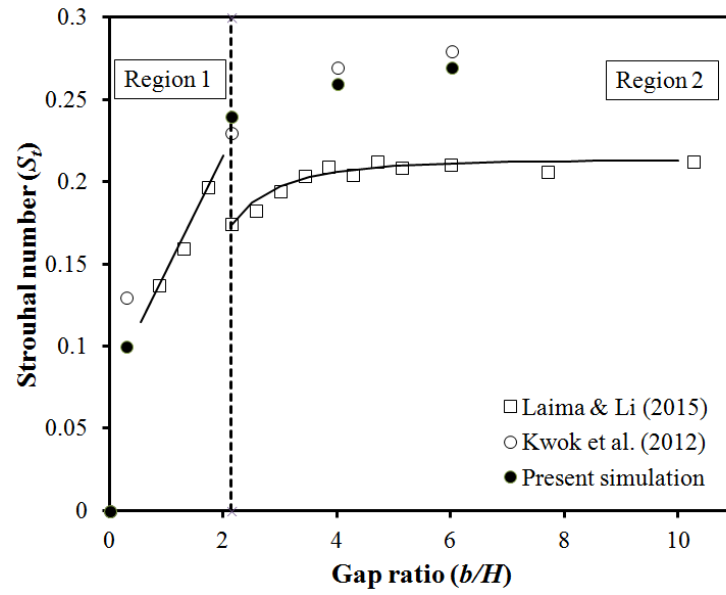
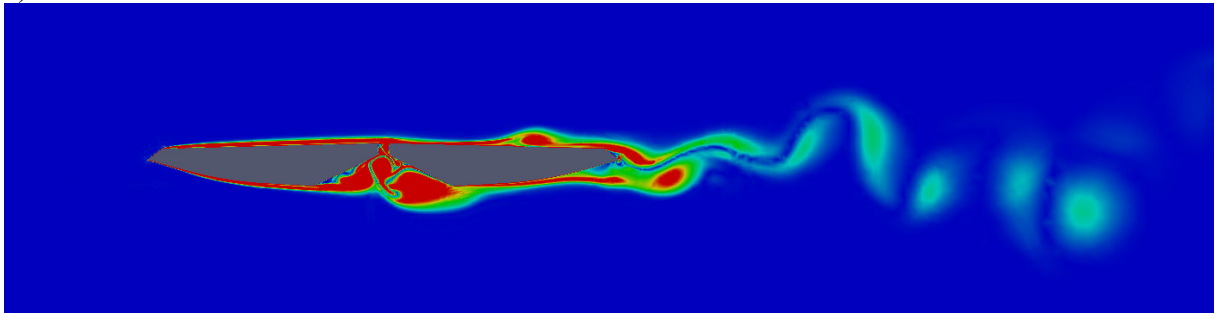


Figure 4. Strouhal number vs. Gap ratio.

a)



b)

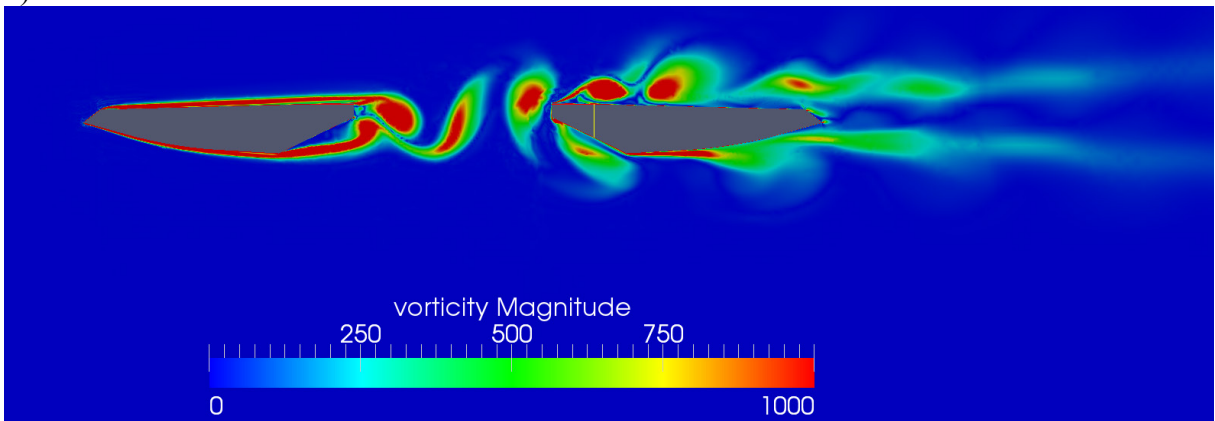


Figure 5. Flow structure for a) Gap 2 (Region 1) and b) Gap 4 (Region 2).

6. PRESSURE DISTRIBUTION AROUND THE BRIDGE DECK

The measurement of pressures around bluff bodies provides a clear picture of their aerodynamic behaviour. The mean pressure distribution allows the identification of flow separation regions while fluctuating pressure distributions permit the identifying separation and reattachment zones or the effect on the downstream box of the signature turbulence originated at the upstream box. Time-averaged and standard deviation pressure coefficients are defined as follows:

$$C_{\bar{p}} = \frac{\bar{p}}{\frac{1}{2}\rho U^2} \quad (7)$$

$$C_{\sigma_p} = \frac{\sigma_p}{\frac{1}{2}\rho U^2} \quad (8)$$

Where \bar{p} is the time-average of the surface pressure time histories at the sampled locations, and σ_p is the standard deviation. One of the strong points of the CFD approach is the ability to continuously monitor and store pressure or other variables of interest along the simulation. In the following the results obtained from 63 points on each box are reported. In order to be consistent with the experimental data in [7] the magnitudes of mean and fluctuating pressure coefficients are scaled with respect to the deck depth H . Negative pressures are depicted outside of the bridge deck, while positive ones are plotted on the inside.

Comparing the numerical results with the wind tunnel tests some differences can be seen. Paying attention in first place to the mean pressure coefficients distribution (figure 6), the agreement obtained for *Gap 1* and *Gap 2*, which are the gaps inside *Region 1*, is remarkable. In *Region 1* the deck cross-section behaves as a single bluff body and since there are not impinging vortices on the leeward deck, the mean pressure coefficients distribution is very accurate. For *Gap 3*, *Gap 4* and *Gap 5*, which are the ones inside *Region 2*, an overestimation of negative pressures on the upper surface of the downstream boxes is apparent.

It must be borne in mind that 2D URANS simulations typically provide unrealistic smooth and periodic simulations, and are equivalent to 3D simulations showing perfect correlation in the span-wise direction. Further explanations can be found in [13]. As a consequence, in numerical simulations, the vortices colliding on the leeward deck roll-up over the upper surface of the deck providing higher mean negative pressures and also higher fluctuating pressures as can be seen in figure 7, where the pressure fluctuations on the leeward boxes are overestimated in all the cases. However, this does not compromise the ability of the numerical simulations to qualitatively simulate the phenomena.

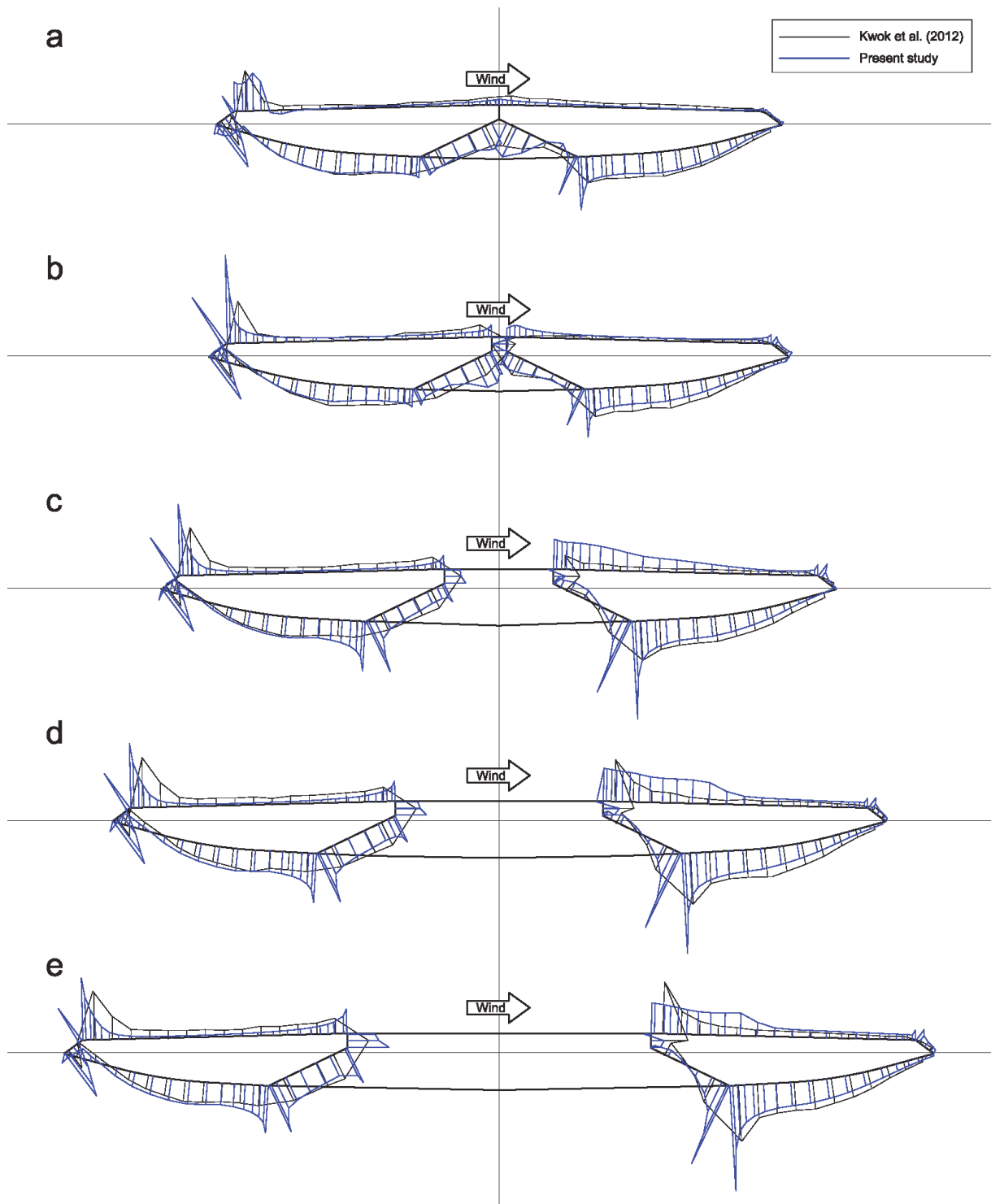


Figure 6. Time-averaged pressure coefficients distribution.

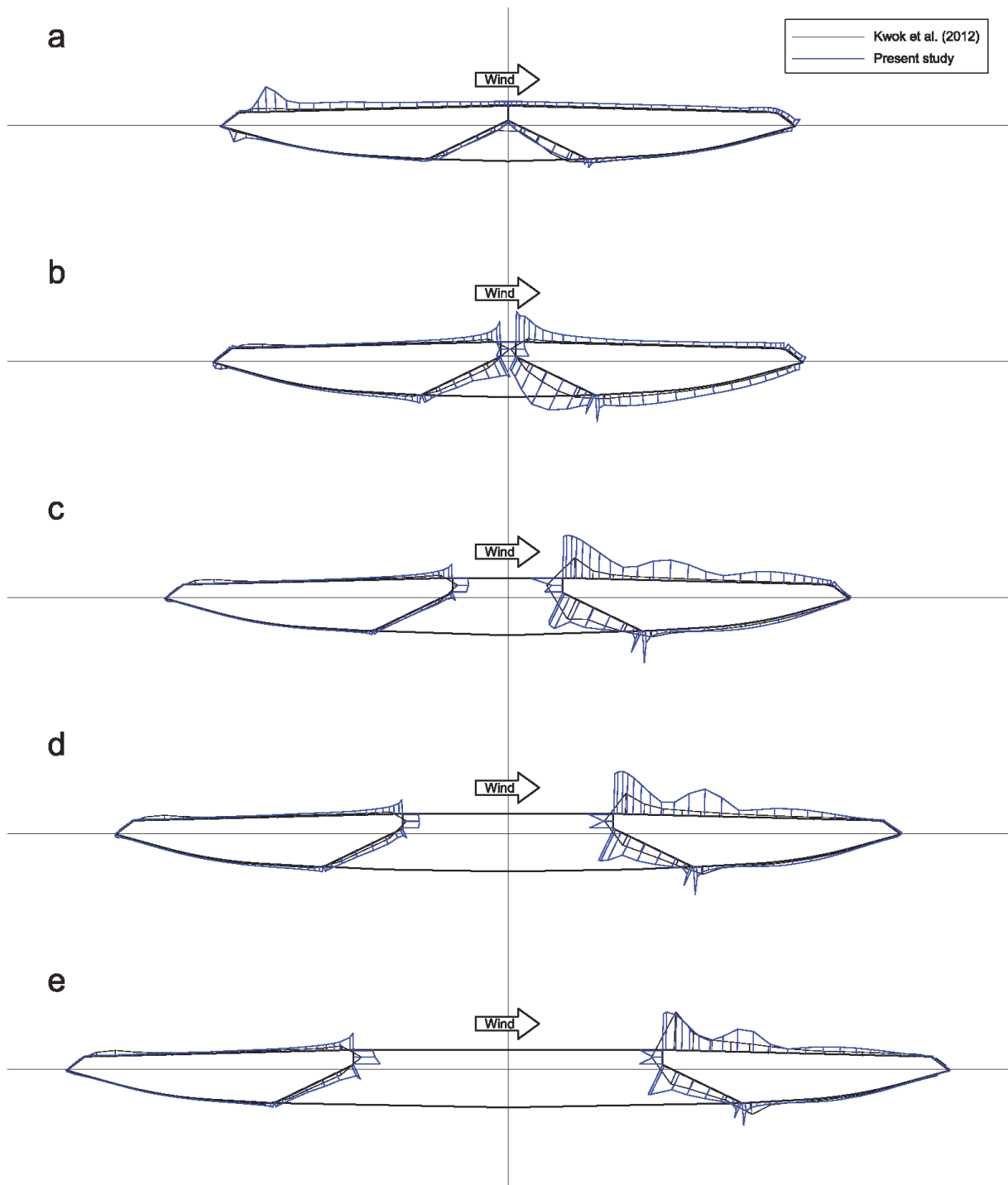


Figure 7. Standard deviation of the pressure coefficients distribution.

In figure 8, the distribution around the deck of the mean and the standard deviation of the pressure coefficients is provided for a 10° angle of attack. In spite of the difficulties in

numerically simulate this strong angle of attack due to the massive flow separation that takes place, the mean pressure coefficients show a good agreement with the wind tunnel data and even the standard deviation distribution is qualitatively correct, in spite of the already mentioned drawbacks of the 2D URANS $k-\omega$ SST model adopted.

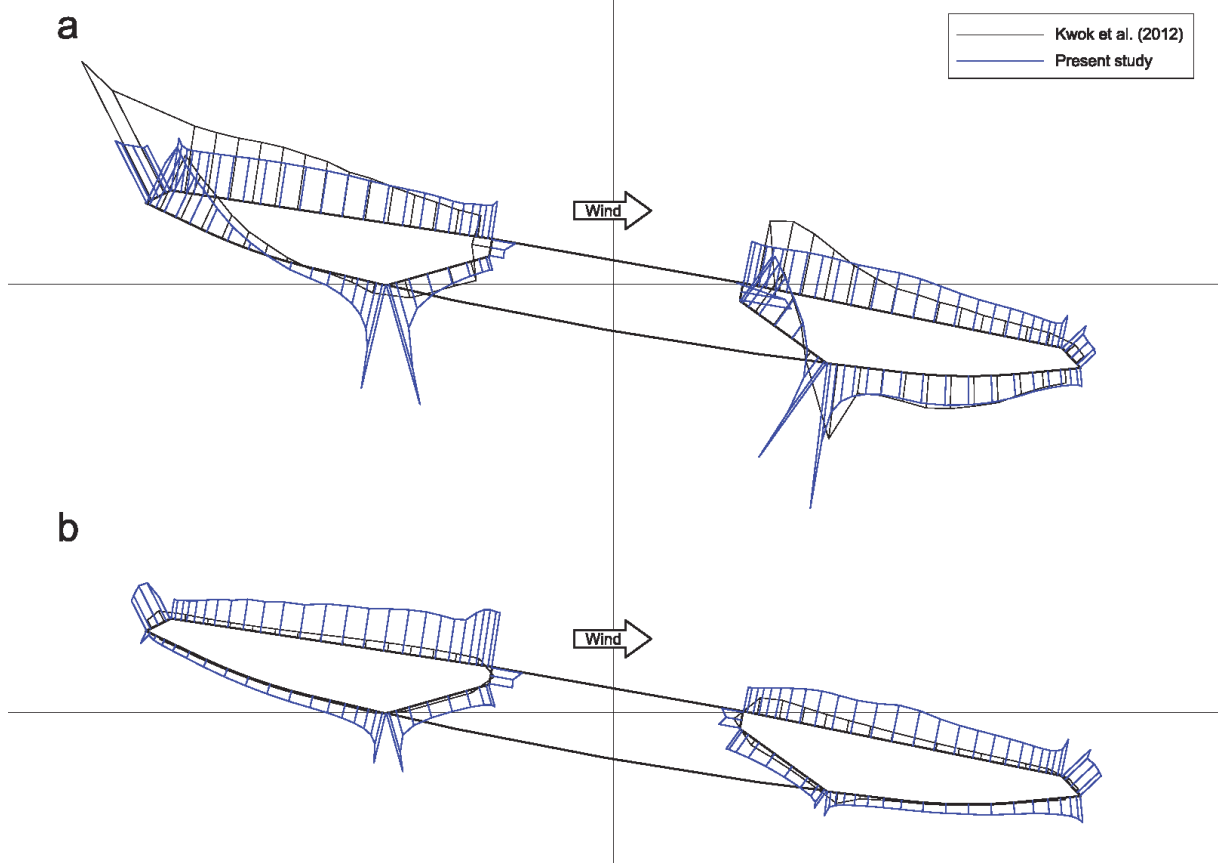


Figure 8. Time-averaged and standard deviation of the pressure coefficients distribution for 10°.

7. CONCLUSIONS

- The motivation for studying the aerodynamic response of twin box bridge decks has been explained.
- The main characteristics of the 2D URANS simulations developed in the frame of the current research have been explained.
- It has been emphasized that the primary purpose of this study is evaluating the capability of this relatively inexpensive simulations to capture the mean features of the flow around twin-box decks as a function of the gap width.
- The numerical simulations have shown a good agreement with the experimental force coefficients for the 5 different gaps considered herein.
- The accuracy in the evaluation of the vortex shedding frequency is remarkable since

both *Region 1* and *Region 2* flow patterns have been identified while the Strouhal number is very close to the experimental data.

- The distributions of the time-averaged and standard deviation pressure coefficients around the deck agree qualitatively with the wind tunnel data.
- This piece of research show the potential of CFD based techniques in the early design stages of long span bridge projects.

ACKNOWLEDGMENTS

This piece of research has been partially financed by the Galician Government (including FEDER funding) with reference GRC2013-056 and by the Spanish Minister of Economy and Competitiveness (MINECO) with reference BIA2013-41965-P. The authors fully acknowledge the received support.

The images of experimental data in figures 6, 7 and 8 are reused from [7], with permission from Elsevier.

REFERENCES

- [1] K. Ogawa, H. Shimodoi and T. Oryu, “Aerodynamic characteristics of a 2-box girder section adaptable for a super-long span suspension bridge”, *J. Wind Eng. Ind. Aerodyn.* Vol. **90**, pp. 2033-2043, (2002).
- [2] G.L. Larose, S.V. Larsen, A. Larsen, M. Hui and A.G. Jensen, *Sectional model experiments at high Reynolds number for the deck of a 1018 m span cable-stayed bridge*. D.A. Smith and C.W. Letchford eds. *11th International Conference on Wind Engineering* (2003).
- [3] G. Diana, F. Resta, M. Belloli and D. Rocchi, “On the vortex shedding forcing on suspension bridge deck”, *J. Wind Eng. Ind. Aerodyn.* Vol. **94**, pp. 341-363, (2006).
- [4] Y. Ge, Y. Yang and F. Cao, *VIV sectional model testing and field measurement of Xihoumen Suspension Bridge with twin box girder*. *13th International Conference on Wind Engineering* (2011).
- [5] X.R. Qin, K.C.S. Kwok, C.H. Fok, P.A. Hitchcock and Y.L. Xu, “Wind-induced self-excited vibrations of a twin-deck bridge and the effects of gap-width”, *Wind Struct.* Vol. **10**(5), pp. 463-479, (2007).
- [6] X.R. Qin, K.C.S. Kwok, C.H. Fok and P.A. Hitchcock, “Effects of frequency ratio on bridge aerodynamics determined by free-decay sectional model tests”, *Wind Struct.* Vol. **12**(5), pp. 413-424, (2009).
- [7] K.C.S. Kwok, X.R. Qin, C.H. Fok and P.A. Hitchcock, “Wind-induced pressures around a sectional twin-deck bridge model: Effects of gap-width on the aerodynamic forces and vortex shedding mechanisms”, *J. Wind Eng. Ind. Aerodyn.* Vol. **110**, pp. 50-61, (2012).
- [8] S. Laima and H. Li, “Effects of gap width on flow motions around twin-box girders and vortex-induced vibrations”. *J. Wind Eng. Ind. Aerodyn.* Vol. **139**, pp. 37-49, (2015).
- [9] T. Vejrum, D.J. Queen, G.L. Larose and A. Larsen, “Further aerodynamic studies

- of Lions' Gate Bridge – 3 lane renovation". *J. Wind Eng. Ind. Aerodyn.* Vol. **88**, pp. 325-341, (2000).
- [10] F. Nieto, S. Hernández, J.Á. Jurado and A. Baldomir, "CFD practical application in conceptual design of a 425 m cable-stayed bridge". *Wind Struct.* Vol. **13**(4), pp. 309-326, (2010).
- [11] J. Balzek, *Computational fluid dynamics: principles and applications*, Elsevier, 2nd Edition, (2005).
- [12] A. Larsen, M. Savage, A. Lafrenière, M.C.H. Hui and S.V. Larsen, "Investigation of vortex response of a twin box bridge section at high and low Reynolds numbers" *J. Wind Eng. Ind. Aerodyn.* Vol. **96**, pp. 934-944, (2008).
- [13] F. Nieto, D.M. Hargreaves, J.S. Owen and S. Hernández, "On the applicability of 2D URANS and SST $k-\omega$ turbulence model to the fluid-structure interaction of rectangular cylinders", *Engineering Applications of Computational Fluid Mechanics*, doi:10.1080/19942060.2015.1004817 (2015).